Detection of Liver Cancer Using Modified Fuzzy Clustering and Decision Tree Classifier in CT Images[1]

Amita Das[a], Priti Das[b], S. S. Panda[c], and Sukanta Sabut[d,*]

[a] *Department of Electronics and Communication Engineering, SOA Deemed to be University, Odisha, India*
[b] *Department of Pharmacology, SCB Medical College and Hospital, Odisha, India*
[c] *Department of Surgical Oncology, IMS & SUM Hospital, SOA Deemed to be University, Odisha, India*
[d] *School of Electronics Engineering, KIIT Deemed to be University, Odisha, India*
** e-mail: sukanta207@gmail.com*

Abstract—Manual detection and characterization of liver cancer using computed tomography (CT) scan images is a challenging task. In this paper, we have presented an automatic approach that integrates the adaptive thresholding and spatial fuzzy clustering approach for detection of cancer region in CT scan images of liver. The algorithm was tested in a series of 123 real-time images collected from the different subjects at Institute of Medical Science and SUM Hospital, India. Initially the liver was separated from other parts of the body with adaptive thresholding and then the cancer affected lesions from liver was segmented with spatial fuzzy clustering. The informative features were extracted from segmented cancerous region and were classified into two types of liver cancers i.e., hepatocellular carcinoma (HCC) and metastatic carcinoma (MET) using multilayer perceptron (MLP) and C4.5 decision tree classifiers. The performance of the classifiers was evaluated using 10-fold cross validation process in terms of sensitivity, specificity, accuracy and dice similarity coefficient. The method was effectively detected the lesion with accuracy of 89.15% in MLP classifier and of 95.02% in C4.5 classifier. This results proves that the spatial fuzzy c-means (SFCM) based segmentation with C4.5 decision tree classifier is an effective approach for automatic recognition of the liver cancer.

Keywords: liver cancer, computed tomography, hepatocellular carcinoma, metastatic carcinoma, segmentation, classifier

DOI: 10.1134/S1054661819020056

1. INTRODUCTION

Prevention and treatment of liver cancer is one of the major focus of research in clinical diagnosis system [1]. The hepatocellular carcinoma and metastatic carcinomas are some well-known class of liver diseases which can be recognized using computer aided diagnosis system [2]. Isolation of cancerous portion using segmentation algorithm is essential for diagnosis of cancers. The detection of malignant tissue is quite difficult due to structural changes in liver with age, sex, body shape, and also the low contrast between normal and malignant tissues. Discrimination of hepatocellular carcinoma from metastatic carcinoma in liver may be difficult because they both appear as moderate to poorly differentiated tumors. Hepatocellular carcinoma is one of the common primary growth of the liver in adults, whereas liver is one of the common sites for metastatic disorder accounting for 25% of all metastasis to the organ. The metastatic carcinoma showed multiple lesions whereas HCC cases are reverse to that. The feature vector generated from the LBP Fourier features are fed to classifiers separately [1–3]. The automated system uses advanced imaging modalities and able to detect the diseases with better accuracy [3, 4]. Lesion segmentation, feature extraction, and disease classification are some of the popular stages of automated detection system. Various standard state-of-art method includes thresholding, clustering, contour and region based models, and machine learning algorithms have been reported to segment the cancerous tissues [5–8].

In a semiautomatic approach, Moltz et al. [6] used the thresholding with morphological processing to obtain the metastatic areas in liver. Chen et al. [7] presented a automated framework that utilizes algorithm for boundary detection for automatic recognition of the liver cancer and a neural network classifier with spatial gray-level co-occurrence matrix based features have been used effective classification of normal, hepatoma and hemangioma types of cancer. Gletsos et al. [8] classified healthy tissue, cyst, hemangioma and hepatocellular carcinoma categories of liver tumor using feed forward neural networks in 48 extracted texture features. Zhang et al. [9] presented an automatic

[1] The article is published in the original.

Received November 13, 2018; revised December 21, 2018; accepted January 20, 2019

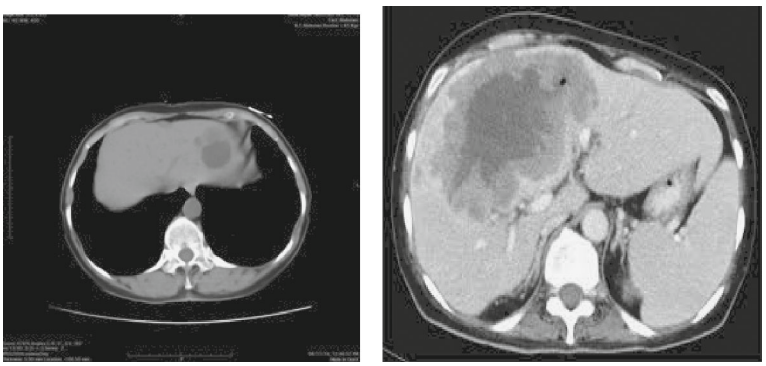

Fig. 1. An example of hepatocellular carcinoma and metastasis carcinoma slices.

detection method based on edge detection and image subtraction to identify hepatocellular carcinoma structure. The cancer types was classified successfully with a three layer NN classifier using integrated feature vector and GLCM feature sets. Sethi et al. [10] reported a CAD system using machine learning technique for the classification of abdominal diseases using 120 CT scan images. They classified the diseases using discrete curve-let transform along with neural network classifier which yielded a highest classification accuracy of 95.1%. In an extension to their work, Sethi et al. [11] presented a better method using new stopping function which was constructed using distance regularized level set evolution for detecting low-contrast cancerous regions in CT images.

Kumar et al. [12] applied different feature extraction methods to classify liver diseases and obtained an accuracy of 96.7% with contourlet texture features. Sun et al. [13] reported multi-channel fully convolutional network (MC-FCN) to separate the tumor from multiphase CT image and validated using manual delineation of experts [12]. Baazaoui et al. [14] presented a semi-automatic entropy based fuzzy region growing approach to separate single and multiple tumors from liver CT scan images. Mostafa et al. [15] presented an artificial bee colony (ABC) based optimization technique to segment the CT images of liver. Further the segmented liver region is refined by region growing approach and achieved an accuracy of 93.73% with similarity index judgment. In a combined approach, Koley et al. [16] reported an entropy based thresholding and granular computing to differentiate the tumor followed by classification using random forest classifier. Chang et al. [17] presented a region growing approach to segment liver tumor and classified by a binary logistic regression analyses classifier with an accuracy of 81.69% using statistical, shape based and kinetic curve based features. Smeets et al. [18] proposed a semi-automatic approach for segmenting liver metastasis using level set method which uses statistical pixel classification and the results are outperformed compared manual method in delineating liver tumors. Hoogi et al. [19] proposed an adaptive local window based level set segmentation technique in 233 CT and MRI images to separate the lesions in liver. An improvement of 0.25 ± 0.13 was obtained in dice similarity index measure compared to global level set segmentation. Most of the machine learning methods are more efficient but sensitive to noise hence it is quite tough to detect accurate tumor region [20].

The segmentation and classification framework described in this paper combines two different approaches. Separation of liver was done with adaptive thresholding and the cancerous region was delineated with spatial fuzzy clustering algorithms using CT scan images. Feature extraction is done using local binary pattern histogram Fourier approach and classified with multilayer perceptron and C45 decision tree classifier in order to classify hepatocellular carcinoma and metastases carcinoma types of cancer. The effectiveness of the proposed method was validated and the results were compared with few state-of art methods.

2. METHODS

We have included 63 hepatocellular carcinoma, and 60 metastasis carcinoma cases for evaluation of this study. Figure 1 shows an example of a slice extracted from the patient having cancerous tissue. The CT image includes three types of phases: non-contrast enhanced phase, arterial phase and portal phase. HCC are small lesions and will appear in the arterial phase only whereas MET appears in multiple lesions and occurs in all three phases. The flow diagram of the proposed automated detection method is shown in Fig. 2. It consists lesion segmentation, feature extraction and classification. The cancerous region was segmented using SFCM algorithm subsequently feature were extracted and classified with classifiers.

2.1. Lesion Segmentation

To obtain accurate lesion structure, the segmentation was performed on high contrast CT scan images.

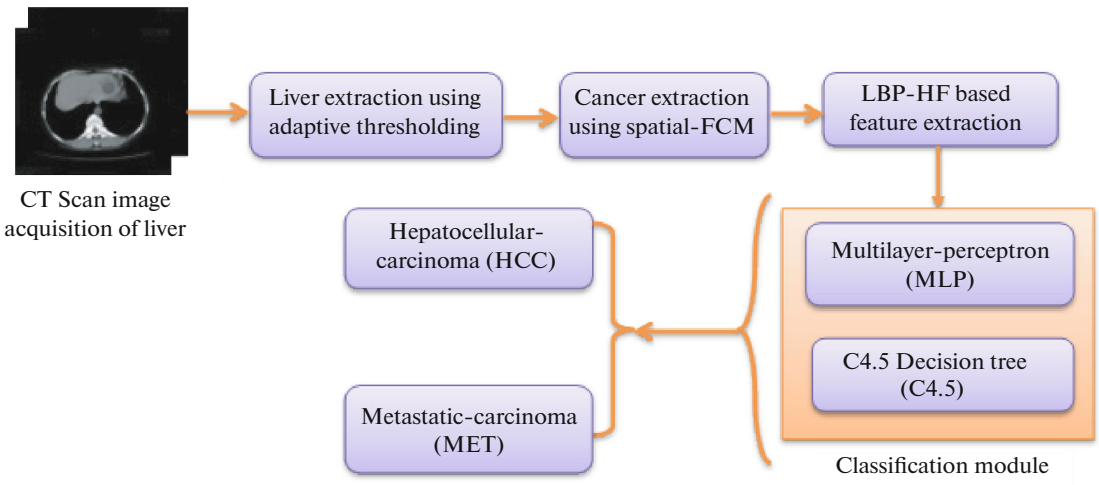

Fig. 2. Flow diagram of the proposed automated liver cancer detection system.

In the CT image, the contrast of the cancerous portion is less compared to other healthy tissues. The abdominal CT images generally consist of liver and some portion of kidney, spleen, etc. So it is necessary to separate the liver from the CT images for which adaptive thresholding was applied. In adaptive thresholding, the histogram of the CT image was analyzed first, thresholding is done using the middle intensity followed by morphological processing that separates the liver portion. The generated liver region is further processed with SFCM approach to segment the cancer lesion.

2.2. Spatial Fuzzy c-Means Clustering

In fuzzy clustering the membership function and the cluster center are deliberated adaptively to reduce a predefined cost function. So FCM is widely applied to medical image segmentation problem. An FCM algorithm employs a membership function, which specifies the degree of membership of the nth object to the m number of cluster.

The cost function of the FCM algorithm is defined in Eq. (1)

$$J = \sum_{n=1}^{N}\sum_{m=1}^{C}\mu_{mn}^{l}\left\|i_n - v_m^2\right\|, \tag{1}$$

where l is the controlling parameter with value ($l > 1$).The membership functions are subject to the subsequent constraints

$$\sum_{m=1}^{C}\mu_{mn} = 1, \quad 0 \le \mu_{mn} \le 1, \quad \sum_{n=1}^{N}\mu_{mn} > 0.$$

The membership function μ_{mn} and the cluster centroids v_m are updated iteratively as in Eqs. (2) and (3).

$$\mu_{mn} = \frac{\left\|i_n - v_m\right\|^{-2/(l-1)}}{\sum_{k=1}^{C}\left\|i_n - v_k\right\|^{-2/(l-1)}}, \tag{2}$$

$$V_i = \frac{\sum_{n-1}^{N}\mu_{mn}^{l} i_n}{\sum_{n=1}^{N}\mu_{mn}^{l}}. \tag{3}$$

The measure problem of standard FCM algorithm is the spatial information are less in segmented image [21, 22]. Chuang et al. [21] presented a spatial fuzzy c-means algorithm where the spatial information is included into the fuzzy membership function as mentioned in Eq. (4).

$$\mu'_{mn} = \frac{\mu_{mn}^{p} h_{mn}^{q}}{\sum_{k=1}^{C}\mu_{kn}^{p} h_{kn}^{q}}. \tag{4}$$

Here p and q are the two controlling parameters and the variables h_{mn} incorporates the spatial information which is given by the Eq. (5)

$$h_{mn} = \sum_{k=N_n}\mu_{nk}. \tag{5}$$

In this case N_n indicate a local window throughout the image pixel n. The membership function μ_{mn} and the centroid V_m are updated as per the Eqs. (2) and (3).

2.3. Local Binary Pattern Based Feature Extraction

Local binary pattern (LBP) is a simple and effective technique for extracting texture features through an image [23]. First of all a spatial neighborhood is selected from an image. In this neighborhood the

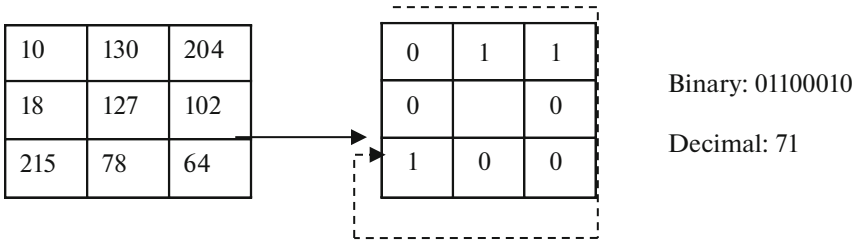

Fig. 3. Basic LBP operator.

intensity of the center pixel is compared with the intensity of the other points presented in the neighborhood. The comparison is done using Eq. (6)

$$LBP_{P,R} = \sum_{i=0}^{P-1} S(g_i - g_c)2^i S(x) = \begin{cases} 1 & x \geq 0 \\ 0 & x < 0. \end{cases} \quad (6)$$

Here P indicate the total no of neighborhood pixels, R represents the radius between center pixel and neighborhood pixel, g_i is the intensity of surrounding neighborhood pixel, and g_c is the intensity of center pixel. Figure 3 shows the basic LBP operator.

The main idea of this method is the thresholding a 3 × 3 neighborhood and the results are shown in a binary no. The histograms of the no of labels are used as texture descriptor. The resultant LBP operator is then extended to an uniform pattern LBP operator where the LBP contain at most two bit wise transition that is from 0 to 1 or vice versa. The numerical example of uniform patterns are 00010000 and 0100100. For simplicity of computation we consider only the uniform patterns, so that the descriptor will reduce to 59 bins. In the uniform LBP histogram, rotation of input image by $k \times 45°$ causes a cyclic shift by k along each row.

2.3.1. LBP histogram Fourier features. According to the property, that states rotation contain shift in the polar representation (P, R) of the surrounding neighborhood, a sets of features are proposed that are invariant to rotation and these features computed from input histogram rows [24]. Discrete Fourier Transform is used to build up these type of features. Let $H(n, \cdot)$ will be the DFT of nth row of the histogram $h_I(U_P(n,r))$, i.e., defined in Eq. (7)

$$H(n,u) = \sum_{r=0}^{P-1} h_I(U_P(n,r))e^{-i2\pi ur/P}, \quad (7)$$

where $U_P(n,r)$ are uniform LBP patterns, n is a number of 1 bits in the pattern, r is rotation of the pattern, P is a number of neighboring sampling points.

According to the DFT rules a cyclic change of the input vector can cause a phase change in DFT coefficient. If $(U_P(n,r)) = h(U_P(n,r-a)$, h' then $H'(n,u) = H(n,u)e^{\frac{-i2\pi ua}{P}}$. And hence, with any $1 < n_1$, $n_2 \leq p-1$ the DFT is presented in Eq. (8)

$$H'(n_1,u)\bar{H}'(n_2,u) = H(n_1,u)e^{\frac{-i2\pi ua}{p}}\bar{H}'(n_2,u)e^{\frac{i2\pi ua}{P}} = H(n_1,u)\bar{H}(n_2,u). \quad (8)$$

Here $\bar{H}(n_2,u)$ represents the complex conjugate of $H(n_1,u)$.

With any $1 < n_1$, $n_2 \leq P-1$, and $0 \leq u \leq p-1$, are represented with the Eq. (9)

$$\mathrm{LBP}^{u2} - \mathrm{HF}(n_1,n_2,u) = H(n_1,u)\bar{H}(n_2,u). \quad (9)$$

The Fourier magnitude contains a subset of LBP feature vector given in Eq. (10)

$$|H(n,0)| = \sum_{r=0}^{P-1} h_I(U_P(n,r)) = h_{\mathrm{LBP}^{riu2}}(n). \quad (10)$$

Here LBP-HF descriptor is used to extract 38 most efficient features for texture classification.

2.4. Classification

The informative feature were extracted from the segmented cancer lesion and classified as HCC and MET using multilayer perceptron and decision tree classifiers.

2.4.1. Multi-layer perception classifier. Multi-layer perception is one of the most popular feed forward NN architecture which is used for both classification and regression purpose [25, 26]. MLP networks are consisting of several layers of nodes and have unidirectional connection. MLP networks are based on N-dimensional input vector and M-dimensional output vector d. So MLP is a function of $y(x, w)$, where w represents the adaptive weight vectors. The error signal actuated from the system controls the learning algo-

rithm. The minimization of error function of MLP learning algorithm is based on the learning set (x_i, d_i), where $i = 1, 2...N$ uses the Euclidian norm of Eq. (11)

$$E(w) = \frac{1}{2}\sum_{i=1}^{N} y(x_i, w) - d_i^2. \quad (11)$$

The error minimization causes the optimal values of weights. The weight adaptation in all gradient based algorithms is generally performed with step by step manner as given in Eq. (12)

$$w(k+1) = w(k) + \gamma p(k), \quad (12)$$

where $p(k)$ is the direction of minimization, γ and w represents the learning and adaptation coefficient. One of the effective minimization algorithms is Levenberg–Marquardf approach where the least square formula is exploited in Eq. (13)

$$E(w) = \frac{1}{2}\sum_{i=1}^{M} (y_i(w) - d_i)^2. \quad (13)$$

This is solved using the second order Newton equation given bellow.

Where $g(k) = \dfrac{\partial E}{\partial W(k)}$ is the gradient of error function of Eq. (24) and $G(k)$ represents the Hessian approximation, which is determined by using Jacobian matrix $J(k)$ presented in Eq. (14)

$$G(k) = J(k)^T J(k) + v. \quad (14)$$

In the above equation the Jacobian matrix J represents the value $J = \dfrac{\partial e}{\partial w}$ and e is defined as $e = [y_i(w) - d_i, ..., y_M(w) - d_M]^T$.

The Levenberg–Marquardf parameters e is adjusted step by step to minimize Hessian G.

2.4.2. Decision tree classifier. Recognition of different diseases is most essential in the field of medical diagnosis for appropriate treatment. The recent decision tree classifier called C4.5 is a suitable choice for classification of medical data. This hierarchical classifier plays an important role in effective classification of data sets. Quinlan presented the C4.5 algorithm in 1993, which is an extension of ID3 (Iterative Dichotomiser 3) algorithm [27]. C4.5 has been marked as a standard machine learning tool for supervised classification and also been widely used as a data analysis model for different areas. The construction of the tree begins at the root node and expanded in a top down approach. In this process each attribute is assessed using a statistical analysis to decide how accurately it can categorize the training samples. The leading attribute is chosen as the root node of the tree. A successor of the main root node is created if it is a discrete valued attribute. Then the training data are stored according to the suitable successor node. This searching procedure is repeated again and again to select the leading attribute for the training samples. This process forms a greedy search for the decision tree approach and it never back tracks to review the previous nodes. When all the samples which are allocated to the one node belongs to the same class at that time the tree stops to add the nodes to it. A new node is initiated from the parent tree only when there are enough samples are left from the sorting. After the complete construction of the tree a tree pruning is commonly executed to avoid over fitting of data.

The C4.5 algorithm uses a statistical test to assign the attributes to each node based on entropy measure. According to the highest information gain ratio the attributes are selected to construct the tree. The information gain ratio that is *Gain Ratio*(A, S) of an attribute, a proportional to the sample set S is represented as

$$Gain\,Ratio(A,S) = \frac{Gain(A,S)}{Spilt\,Information(A,S)}, \quad (15)$$

where $Gain(A,S) = Ent(S) - \sum_{a\in A}\dfrac{|S_a|}{|S|} Ent(S_a)$ and $Split\,Information(A,S) = -\sum_{a\in A}\dfrac{|S_a|}{|S|}\log_2\dfrac{|S_a|}{|S|}$.

Here S_a is the subset of S. The information gain ratio can be calculated directly for discrete valued attributes; on the other hand continuous valued attributes are required to be discretized for the calculation of information gain ratio.

2.5. Validation of the Study

The extracted feature were divided into training and testing data sets. The K-fold cross validation was used to validate the performance of the classifier. During this validation process the original data set was randomly divided into k-equal size sub-sets. A single sub-sample is chosen from the k-samples which were used as testing data and the remaining $k - 1$ sub samples were used as training data. The outcomes of the k-folds are averaged together to produce a single result. To estimate the performance of classifiers, confusion matrix is formed which represents preferred and classified outcomes produced by the classifiers. Four cases have been created i.e., True positive (TP), True negative (TN), False positive (FP), False negative (FN). The result of MLP and decision tree classifiers to clas-

Table 1. Classification results of SFCM using MLP and C4.5 decision tree classifier

No. of folds		Specificity, %	Sensitivity, %	Accuracy, %	DSC, %	ROC area
2	MLP	82.61	88.42	85.45	85.42	85.20
	C4.5	98.41	91.66	95.10	90.90	96.70
3	MLP	88.90	86.73	87.81	87.41	90.00
	C4.5	100	86.67	93.49	92.85	93.70
4	MLP	84.22	90.01	86.94	87.00	85.20
	C4.5	93.65	88.30	91.05	90.59	91.70
5	MLP	88.91	85.00	87.05	86.52	85.20
	C4.5	93.65	95.01	94.30	94.21	94.30
6	MLP	87.32	95.00	91.01	91.21	91.70
	C4.5	96.87	96.67	96.74	96.67	97.20
7	MLP	87.32	90.00	88.62	88.60	86.30
	C4.5	87.31	95.01	91.05	91.20	95.30
8	MLP	90.40	93.31	91.81	91.84	92.10
	C4.5	98.41	98.34	98.37	98.34	98.40
9	MLP	90.40	93.31	91.81	91.84	88.90
	C4.5	98.41	98.34	98.37	98.34	98.20
10	MLP	92.06	91.66	91.86	91.66	91.80
	C4.5	98.42	95.01	96.74	96.62	96.70
Avg.	**MLP**	**88.01**	**90.38**	**89.15**	**89.05**	**88.48**
	C4.5	**96.12**	**93.89**	**95.02**	**94.41**	**95.8**

sify cancerous lesions are presented using different measures as given Eqs. (16)–(19)

$$\text{Sencitivity} = \frac{\text{TP}}{\text{TP} + \text{FN}}, \tag{16}$$

$$\text{Specificity} = \frac{\text{TN}}{\text{TN} + \text{FP}}, \tag{17}$$

$$\text{Accuracy} = \text{TP} + \text{TN}/(\text{TP} + \text{TN} + \text{FP} + \text{FN}), \tag{18}$$

$$\text{Dice similarity cofficient (DSC)} = 2\text{TP}/(2\text{TP} + \text{FP} + \text{FN}). \tag{19}$$

3. ANALYSIS OF RESULTS

Initially, the liver was separated from other parts of body with adaptive thresholding and the resultant image is further processed for detection of cancer region using SFCM algorithm. The segmented cancerous lesions were separated from normal tissue in CT scan images of liver as shown in Figs. 4 and 5 for HCC and MET class cancer respectively. The final structure of delineated cancer lesion is shown in Figs. 4d and 5d. From the visual observation of the delineated result, it was observed that the SFCM algorithm could effectively extract the cancerous region with exact structure having distinct boundary having low PSNR value of 23.196 and high MSE value of 311.517. The proposed approach includes the classification results of cancer liver using SFCM algorithm. The process of cross validation is iterating up to 10 number of times (10-folds). Table 1 shows the sensitivity, specificity, accuracy, and DSC results of MLP and decision tree classifier in each fold at 10-fold cross validation process. It was observed from the table that the decision tree clas-

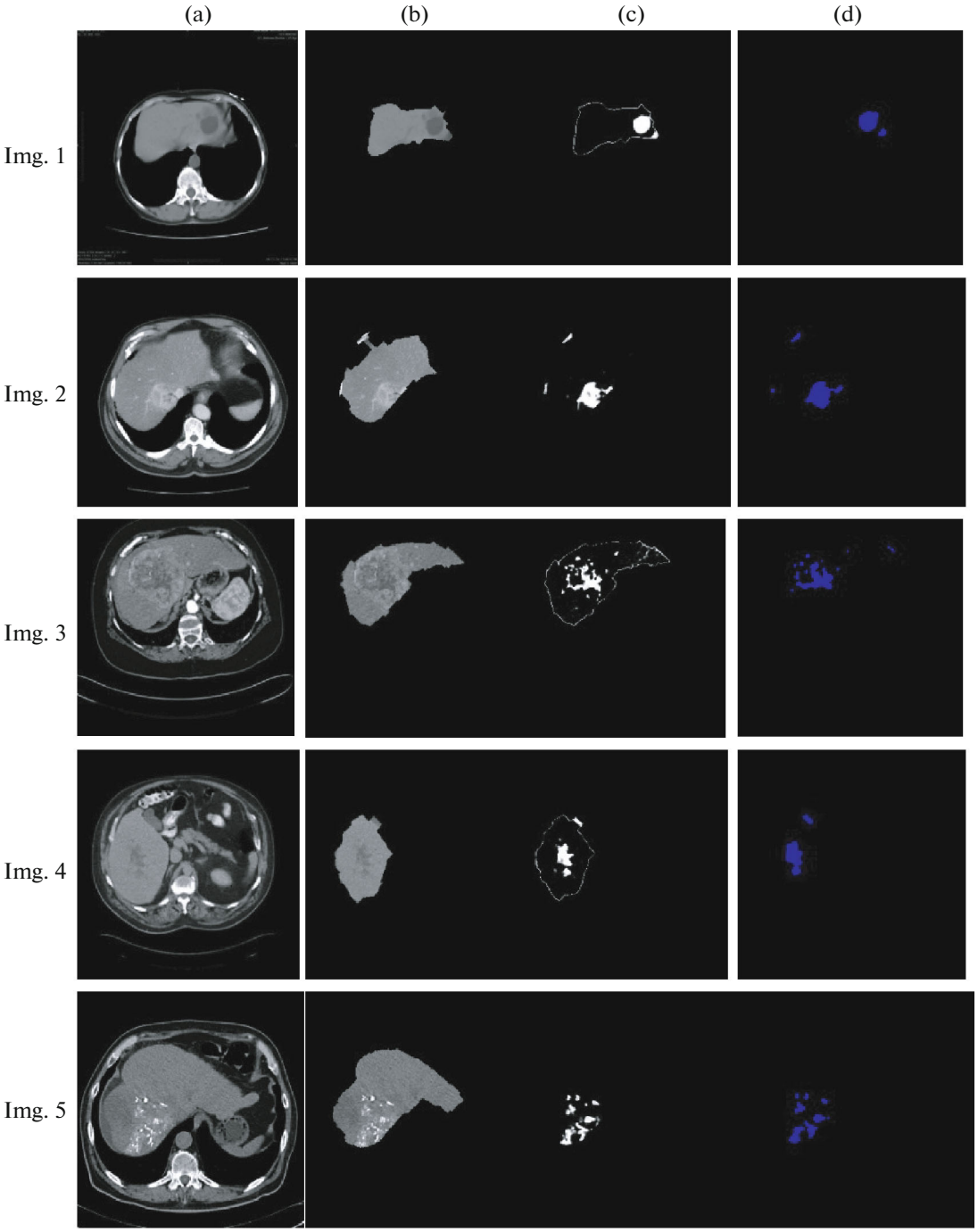

Fig. 4. Examples of segmented results of hepatocellular carcinoma (a) original HCC image; (b) segmented liver image; (c) segmented ROI using SFCM; (d) final result after morphological operation.

sifier achieved better accuracy with average value of 95.02% compared to MLP classifier which is having average accuracy of 89.15%. The performance plots of accuracy and ROC curve are shown from Figs. 6 and 7. Figure 8 shows the comparative results obtained from the test sets in cross validation process for two classifiers. From the plots, we concluded that the detection and classification of hepatocellular carcinoma and metastasis carcinoma types of liver cancer using CT images can be effectively done using C4.5 classifier in spatial FCM based segmentation approach.

4. DISCUSSION

The proposed methodology gives a feasible way to tackle with automatic medical image segmentation and diseases classification problem. This technique is

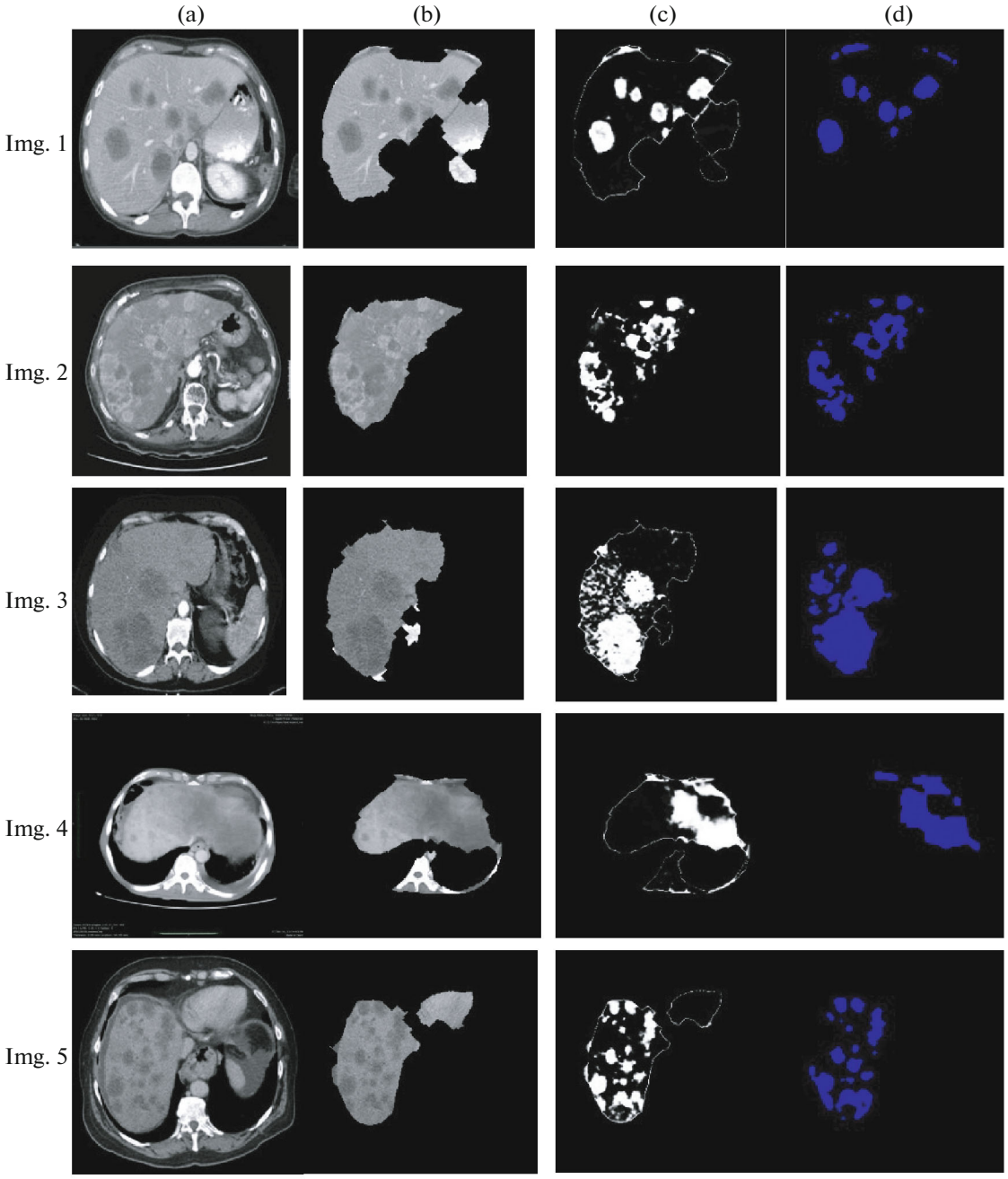

Fig. 5. Examples of segmented results of metastatic carcinoma; (a) original metastatic image; (b) segmented liver image; (c) segmented output; (d) final result after morphological operation using SFCM algorithm.

test on different CT images of patients having hepatocellular carcinoma and metastatic carcinoma types of liver cancer. An automatic lesion segmentation was achieved using spatial fuzzy c-means clustering that delineates the affected area. The study proceeds with different classifiers performance with a set of extracted feature vectors and was classified with MLP and C4.5 decision tree classifier. The C4.5 classifier leads an improved performance with LBP-HF texture descriptor compared to the MLP classifier. A comparison table with existing published articles is presented in Table 2. Our method was outperformed all other presented method with better accuracy.

5. CONCLUSIONS

Image segmentation of liver CT scan image is a crucial task as the image comprise some portion of kidney, spleen etc. The contour based and clustering based methods were widely used for medical image

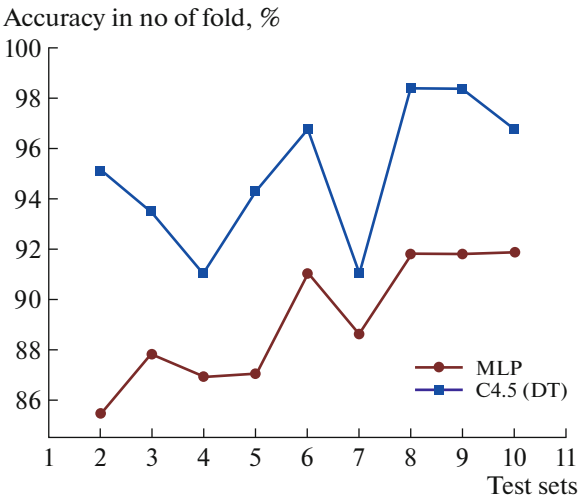

Fig. 6. The accuracy test of MLP and C4.5 classifier for SFCM segmentation algorithm.

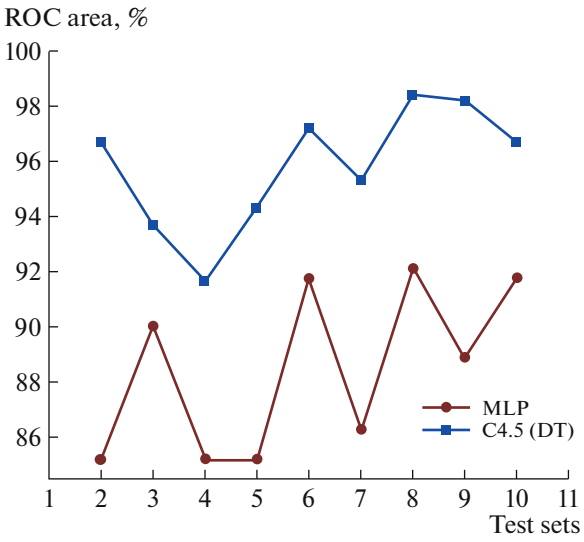

Fig. 7. The ROC curve of MLP and C4.5 classifier for SFCM segmentation algorithm.

segmentation. In this paper, we have presented a hybrid approach that integrates adaptive thresholding and spatial FCM approaches for segmentation of cancer in liver. Initial segmentation was done using adaptive thresholding to segment the liver portion from kidney and spleen and then spatial fuzzy c-means clustering method was proposed to obtain cancer region from liver image. After segmenting the cancerous tissue in SFCM method and a LBP-Fourier feature descriptor was applied to extract features from the segmented tumor images. Finally MLP and C4.5 decision tree classifiers were employed to classify the liver cancer as hepatocellular carcinoma and metastatic carcinoma. Better detection accuracy of 95.02% was achieved in C4.5 classifiers. The result implies that the proposed segmentation approach based on SFCM is able to detect the exact boundary structure and protects the important information of cancer region which help in classifying with better accuracy. The classification procedure provides efficient defection of

Table 2. Comparison of some existing techniques with the proposed technique

Author/year	Modality/classes	Features	Classifier	Accuracy, %
Sethi et al. (2016) [12]	CT/tumor, cyst calculi, normal liver	GLCM, DWT, DCT	ANN	95.1
Chang et al. (2017) [17]	CT/benign, malignant	GLCM shape, kinetic curve based	Binary logistic regression analysis	81.82
Alahmer et al. (2016) [29]	CT/benign, malignant	Intensity, texture, shape features	SVM	89
Mala et al. (2015) [30]	CT/fatty, cirrhosis liver	Wavelet based statistical feature	PNN, LVQ, BPN	PNN–95 LVQ–93 BPN–80
Meng et al. (2014) [31]	MRI/benign type liver tumor (BLT)	Histogram based feature extraction	SVM	86.67
Mittal et al. (2011) [32]	US/Cyst, HCC, hemangioma, normal liver	FOS, GLRLM, TEM, GWT	BPN	86.4
Proposed	**CT/HCC, MET**	**LBP-HF**	**C4.5**	**95.02**

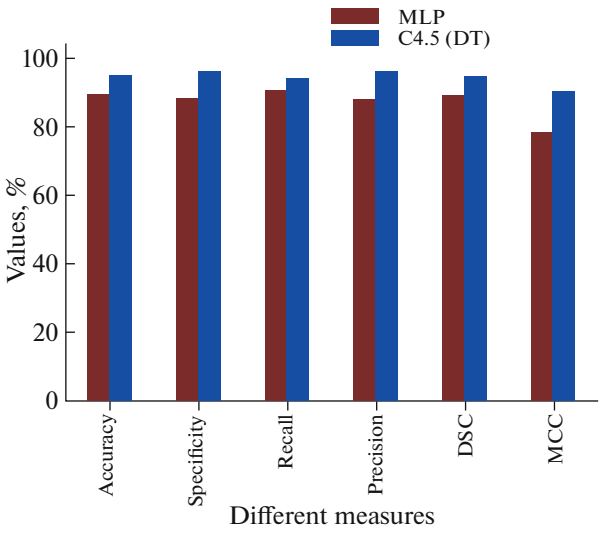

Fig. 8. Comparison of different measures of cancer detection using MLP and C4.5 classifier.

cancer lesion without any intervention of manual process. The method could be useful for the clinicians in diagnosis process of cancer diseases at the early stage.

REFERENCES

1. K. Na, S.-K. Jeong, M. J. Lee, S. Y. Cho, S. A. Kim, M. J. Lee, S. Y. Song, H. Kim, K. S. Kim, H. W. Lee, and Y. K. Paik, "Human liver carboxylesterase 1 outperforms alpha-fetoprotein as biomarker to discriminate hepatocellular carcinoma from other liver diseases in Korean patients," Int. J. Cancer **133** (2), 408–415 (2013).
2. Y. S. Kim, S. Y. Sohn, and C. N. Yoon, "Screening test data analysis for liver disease prediction model using growth curve," Biomed. Pharmacother. **57** (10), 482–488 (2003).
3. T. Murakami, Y. Imai, M. Okada, T. Hyodo, W.-J. Lee, M.-J. Kim, T. Kim, and B. I. Choi, "Ultrasonography, computed tomography and magnetic resonance imaging of hepatocellular carcinoma: Toward improved treatment decisions," Oncology **81 (**Suppl. 1), 86–99 (2011).
4. K. Mitsuzaki, Y. Yamashita, I. Ogata, T. Nishiharu, J. Urata, and M. Takahashi, "Multiple-phase helical CT of the liver for detecting small hepatomas in patients with liver cirrhosis: Contrast-injection protocol and optimal timing," AIR, Am. J. Roentgenol. **167** (3), 753–757 (1996).
5. W. Xie and J. Liu, "Fuzzy c-means clustering algorithm with two layers and its application to image segmentation based on two-dimensional histogram," Int. J. Uncertainty, Fuzziness Knowl.-Based Syst. **2** (3), 343–350 (1994).
6. J. H. Moltz, L. Bornemann, V. Dicken, and H.-O. Peitgen, "Segmentation of liver metastases in CT scans by adaptive thresholding and morphological processing," in *The MIDAS Journal — Grand Challenge Liver Tumor Segmentation* (*2008 MICCAI Workshop*).
7. E.-L. Chen, P.-C. Chung, C.-L. Chen, H.-M. Tsai, and C.-I. Chang, "An automatic diagnostic system for CT liver image classification," IEEE Trans. Biomed. Eng. **45** (6), 783–794 (1998).
8. M. Gletsos, S. G. Mougiakakou, G. K. Matsopoulos, K. S. Nikita, A. S. Nikita, and D. Kelekis, "A computer-aided diagnostic system to characterize CT focal liver lesions: design and optimization of a neural network classifier," IEEE Trans. Inf. Technol. Biomed. **7** (3), 153–162 (2003).
9. X. Zhang, H. Fujita, T. Qin, J. Zhao, M. Kanematsu, T. Hara, X. Zhou, R. Yokoyama, H. Kondo, and H. Hoshi, "CAD on liver using CT and MRI," in *Medical Imaging and Informatics, MIMI 2007*, Ed. by X. Gao, H. Müller, M. J. Loomes, R. Comley, and S. Luo, Lecture Notes in Computer Science (Springer, Berlin, Heidelberg, 2008), Vol. 4987, pp. 367–376.
10. G. Sethi and B. S. Saini, "Computer aided diagnosis system for abdomen diseases in computed tomography images," Biocybern. Biomed. Eng. **36** (1), 42–55 (2016).
11. G. Sethi, B. S. Saini, and D. Singh, "Segmentation of cancerous regions in liver using an edge-based and phase congruent region enhancement method," Comput. Electr. Eng. **53**, 244–262 (2016).
12. S. S. Kumar, R. S. Moni, and J. Rajeesh, "An automatic computer-aided diagnosis system for liver tumors on computed tomography images," Comput. Electr. Eng. **39** (5), 1516–1526 (2013).
13. C. Sun, S. Guo, H. Zhang, J. Li, M. Chen, S. Ma, L. Jin, X. Liu, X. Li, and X. Qian, "Automatic segmentation of liver tumors from multiphase contrast-enhanced CT images based on FCNs," Artif. Intell. Med. **83,** 58–66 (2017).
14. A. Baâzaoui, W. Barhoumi, A. Ahmed, and E. Zagrouba, "Semi-automated segmentation of single and multiple tumors in liver CT images using entropy-based fuzzy region growing," IRBM **38** (2), 98–108 (2017).
15. A. Mostafa, A. Fouad, M. A. Elfattah, A. E. Hassanien, H. Hefny, S. Y. Zhu, and G. Schaefer, "CT liver segmentation using artificial bee colony optimization," in *Proc. 19th Int. Conf. on Knowledge Based and Intelligent Information and Engineering Systems*, Procedia Comput. Sci. **60,** 1622–1630 (2015).
16. S. Koley, A. K. Sadhu, P. Mitra, B. Charkaborty, and C. Charkaborty, "Delineation and diagnosis of brain tumors from post contrast T1-weighted MR images using rough granular computing and random forest," Appl. Soft Comput. **41,** 453–465 (2016).
17. C. C. Chang, H. H. Chen, Y. C. Chang, M. Y. Yang, C. M. Lo, W. C. Ko, Y. F. Lee, K. L. Liu, and R. F. Chang, "Computer-aided diagnosis of liver tumors on computed tomography images," Comput. Methods Programs Biomed. **145** (Issue C), 45–51 (2017).
18. D. Smeets, D. Loeckx, B. Stijnen, B. De Dobbelaer, D. Vandermeulen, and P. Suetens, "Semi-automatic level set segmentation of liver tumors combining a spi-

ral-scanning technique with supervised fuzzy pixel classification," Med. Image Anal. **14** (1), 13–20 (2010).

19. A. Hoogi, C. F. Beaulieu, G. M. Cunha, E. Heba, C. B. Sirlin, S. Napel, and D. L. Rubin, "Adaptive local window for level set segmentation of CT and MRI liver lesions," Med. Image Anal. **37,** 46–55 (2017).
20. W. Li, F. Jia, and Q. Hu, "Automatic segmentation of liver tumor in CT images with deep convolutional neural networks," J. Comp. Commun. **3** (11), 146–151 (2015).
21. K.-S. Chuang, H.-L. Tzeng, S. Chen, J. Wu, and T.-J. Chen, "Fuzzy c-means clustering with spatial information for image segmentation," Comput. Med. Imaging Graphics **30** (1), 9–15 (2006).
22. W. Cai, S. Chen, and D. Zhang, "Fast and robust fuzzy c-means clustering algorithms incorporating local information for image segmentation," Pattern Recognit. **40** (3), 825–838 (2007).
23. S. Abbasi and F. Tajeripour, "Detection of brain tumor in 3D MRI images using local binary patterns and histogram orientation gradient," Neurocomputing **219**, 526–535 (2017).
24. T. Ahonen, J. Matas, C. He, and M. Pietikäinen, "Rotation invariant image description with local binary pattern histogram Fourier features," *Image Analysis, SCIA 2009*, Ed. by A. B. Salberg, J. Y. Hardeberg, and R. Jenssen, Lecture Notes in Computer Science (Springer, Berlin, Heidelberg, 2009), Vol. 5575, pp. 61–70.
25. E. A. Zanaty, "Support Vector Machines (SVMs) versus Multilayer Perception (MLP) in data classification," Egypt. Inf. J. **13** (3), 177–183 (2012).
26. I. Elamvazuthi, N. H. X. Duy, Z. Ali, S. W. Su, M. K. A. Ahamed Khan, and S. Parasuraman, "Electromyography (EMG) based classification of neuromuscular disorders using Multi-Layer Perceptron," Procedia Comput. Sci. **76,** 223–228 (2015).
27. J. R. Quinlan, *C4.5: Programs for Machine Learning* (Morgan Kaufmann, San Mateo, CA, 1993).
28. D. R. Nayak, R. Dash, and B. Majhi, "Classification of brain MR images using discrete wavelet transform and random forests," in *Proc. 2015 5th National Conf. on Computer Vision, Pattern Recognition, Image Processing and Graphics* (*NCVPRIPG*) (Patna, India, 2015), IEEE, pp. 1–4.
29. H. Alahmer and A. Ahmed, "Computer-aided classification of liver lesions from CT images based on multiple ROI," Procedia Comput. Sci. **90,** 80–86 (2016).
30. K. Mala, V. Sadasivam, and S. Alagappan, "Neural network based texture analysis of CT images for fatty and cirrhosis liver classification," Appl. Soft Comput. **32,** 80–86 (2015).
31. D. Selvathi, C. Malini, and P. Shanmugavalli, "Automatic segmentation and classification of liver tumor in CT images using adaptive hybrid technique and contourlet based ELM classifier," in *Proc. 2013 Int. Conf. on Recent Trends in Information Technology* (*ICRTIT*) (Chennai, India, 2013), IEEE, pp. 205–256.
32. D. Mittal, V. Kumar, S. C. Saxena, N. Khandelwal, and N. Kalra, "Neural network based focal liver lesion diagnosis using ultrasound images," Comput. Med. Imaging Graphics **35** (4), 315–323 (2011).

Amita Das is a research scholar in the Department of Electronics and Communication Engineering, Institute of Technical Education and Research, Siksha SOA Deemed to be University Anusandhan University, Odisha, India. She received his B. Tech Degree in Electronics and Communication Engineering from BPUT, Odisha, in 2009 and M. Tech in Communication System Engineering from Siksha SOA Deemed to be University Anusandhan University, Odisha, India in 2011. She has over 4 years of teaching and research experience. She has published research papers in journals and conferences. Her research interest includes signal and image processing.

Priti Das is an Associate Professor in the Department of Pharmacology, SCB Medical College and Hospital, Cuttack, Odisha, India. She is Editor-in-Chief, International Journal of Telemedicine and Clinical Practices, published from Inderscience Publishing House.

Soumya S. Panda received MD in Medicine, DM in Oncology. Presently working as Associate Professor, Department of Medical Oncology IMS & SUM Hospital Bhubaneswar, Odisha. His research concerns diagnosis, monitoring, and screening for cancer.

S.K. Sabut is working as Associate Professor, School of Electronics Engineering, KIIT University, India. He received his Diploma in Rehabilitation Engineering, BE in Electronics and Communication, M. Tech in Biomedical Instrumentation and PhD in Medical Science and Technology from IIT, Kharagpur in 2010. He has over 18 years of experience in both teaching and research. His research interest includes biomedical signal and image processing, neural engineering and biomedical instrumentation. He has published research papers in international journals and conferences. He is a member of IEEE, IFESS, Rehabilitation council of India, and the Institution of Engineers (India).